

Received February 7, 2019, accepted March 7, 2019, date of publication March 18, 2019, date of current version April 5, 2019.

Digital Object Identifier 10.1109/ACCESS.2019.2905869

An Efficient and Reliable QoF Routing for Urban VANETs With Backbone Nodes

LEI LIU¹, (Student Member, IEEE), CHEN CHEN¹, (Senior Member, IEEE), BIN WANG²,
YANG ZHOU³, AND QINGQI PEI¹, (Senior Member, IEEE)

¹State Key Laboratory of Integrated Service Networks, Xidian University, Xi'an 710071, China

²School of Communication Engineering, Xi'an University of Science and Technology, Xi'an 710054, China

³Ministry of Water Resources Information Center, Beijing 100053, China

Corresponding author: Chen Chen (cc2000@mail.xidian.edu.cn)

This work was supported in part by the National Natural Science Foundation of China under Grant 61571338, Grant U1709218, and Grant 61672131, in part by the Key Research and Development Plan of Shaanxi Province under Grant 2017ZDCXL-GY-05-01, in part by the National Key Research and Development Program of China under Grant 2016YFE0123000 and Grant 2017YFE0121400, in part by the Xi'an Key Laboratory of Mobile Edge Computing and Security under Grant 201805052-ZD3CG36, and in part by the 111 Project of China under Grant B08038.

ABSTRACT Because of the dynamic topology, high mobility of nodes, and complicated channel environments in urban areas, existing routings methods are susceptible to frequent link interruptions and channel congestions. To address these issues, a Quality of Forwarding (QoF)-based reliable geographic routing (QFRG) in urban vehicular ad hoc networks (VANETs) is proposed, where the best route is determined by guaranteeing the QoF and satisfying the link reliability requirement. Two theoretical models for QoF and link reliability analysis are first presented. Taking into consideration the transmission cost and the packet delivery ratio, the QoF is, then, employed to provide the quantitative evaluation to the road segments through the presented road weight evaluation (RWE) scheme, which takes into account the impact of the relative position of links on the network performance. Next, to accommodate the network scale of an urban city, the city map is divided into smaller grid zones. Based on the position of the destination, different transmission strategies are presented for packet forwarding. The extensive simulations demonstrate our protocol's superiority in both transmission delay and packet delivery ratio compared with the existing schemes.

INDEX TERMS Vehicular ad hoc networks, quality of forwarding, reliability, routing protocol.

I. INTRODUCTION

Vehicular ad hoc networks (VANETs) have attracted considerable attention for the potential of enhancing road safety and improving driving comfort [1], [2]. By two main communication patterns of vehicle-to-vehicle (V2V) and vehicle-to-infrastructure (V2I) [3] illustrated in Fig. 1, a variety of safety and infotainment applications can be supported, e.g., collision avoidance, social networking and crowdsensing networking [4], [5]. In order to realize these applications, it is crucial to design an efficient and reliable routing to guarantee data transmission. However, several inherent characteristics of VANETs including high node mobility, harsh channel environment and limited network resources impose huge challenges in the routing design [6].

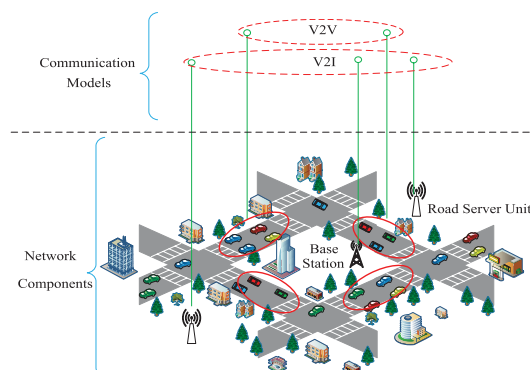


FIGURE 1. Network scenario in VANETs.

The associate editor coordinating the review of this manuscript and approving it for publication was Zhi Liu.

There have been many efforts devoted to the routing design in VANETs, which can be mainly classified into topology-based and position-based. By comparison, position-based

routing represents a promising technique for data transmission in urban VANETs [7]. Generally, urban roads contain two basic parts: intersections and road segments. A position-based routing protocol aims to find the best routing path, which is a series of road segments between two communication nodes. Two important issues arise: how to select road segments to form the routing path, and how to forward data packets along the selected road segments.

Given a pair of communication nodes, multi-hop transmission is used to deliver the packet between them when their distance is beyond the radio range [8]. Due to high mobility in VANETs, the distance between nodes dramatically varies with time. This causes short link lifetime and intermittent network connectivity [9]. In this situation, frequent link partitions often occur, which will disturb the multi-hop data transmission and increase the packet loss ratios. Under this situation, link reliability is a vital consideration for routing design. In [10], a data dissemination scheme is investigated by exploiting the link reliability.

On the other hand, the routing metric plays an important role in determining the optimal route by providing quantifiable values to judge the efficiency of each route [11]. Maxduration-minangle greedy perimeter stateless routing (MM-GPSR) [12] selects the node with the maximum cumulative communication duration as the next hop in greedy forwarding and the node with the minimum angle for relay transmission in perimeter forwarding. Backbone-assisted hop greedy (BAHG) [13] utilizes the number of hops as the guide for routing selection. Stable and delay constraints routing (SDCR) [14] and efficient group key management for secure routing (EGSR) [15] aim to find the optimal routing path by considering the network connectivity. These protocols account for the mobility of nodes, but fail to fully capture the impact of channel status on network performance. Although travel prediction-based data (TPD) [16], and double ruling (MADR) [17] provide the delay model to make routing decisions, they are mainly applied for light traffic environments. Prediction-based reliable and efficient opportunistic routing (PRO) [18] takes into consideration the link quality when selecting the relay node. However, there is the risk of getting the local optimum without global knowledge of traffic conditions. Actually, it is extremely challenging to estimate the link quality in VANETs because of dynamic topology and complicated channel environments. A well-known metric used to measure the link quality is the expected transmission count (ETX) [19]. Hybrid location-based ad hoc routing (HLAR) [20] adopts ad hoc on-demand distance vector (AODV) with the ETX metric to find the route with the best link quality. Long lifetime anypaths (LLA) [21] introduces a special metric of link cost that combines the packet delivery ratio and the level of link stability to reflect the link performance. Although ETX can be explored to evaluate the performance of multi-hop forwarding to some extent, it has some limitations. By definition, ETX knows that an infinite number of transmissions is allowed for the link layer. In this case, the packet is never dropped in the link layer. The ETX

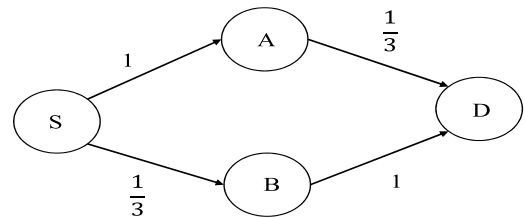


FIGURE 2. Effect of relative link positions on network performance.

value of a path is the sum of the ETX values of all links along the path, which makes the number of retransmissions needed for successful data transmission along the path dependent on each link quality but ignore the positions of these links. A simple example is illustrated in Fig. 2. There are two routing paths from node S to node D, and the number attached to each link represents the packet delivery ratio. Based on the definition of ETX, both *path a* : $S \rightarrow A \rightarrow D$ and *path b* : $S \rightarrow B \rightarrow D$ have the same ETX value, i.e., 4. However, they exhibit different performances. With the assumption that two transmissions per packet are allowed to be performed by the link layer, the probability of a packet passing successfully the last link in *path a* is: $\frac{1}{3} + (1 - \frac{1}{3})(\frac{1}{3}) = 0.55$, which is bigger than the one that a packet passes the last link in *path b*, i.e., 1. It is known from [22] that *path b* is the best choice. The reason is that due to the presence of "bad" link near the destination in *path a*, data packets are more likely to be dropped on that link, resulting in the waste of transmission effort on previous links (i.e., the link between S and A) as well as increased the transmission cost.

In this paper, we propose a quality of forwarding (QoF) based reliable geographic routing for urban VANETs. This protocol aims to find a best routing path that guarantees QoF while satisfying link reliability. The contributions of our work are summarized as follows:

- 1) Two analytical models, i.e., QoF and link reliability, are given as guides for routing selection. The QoF is designed to consider transmission cost, packet delivery ratio as well as relative link positions, while the link reliability is used to reflect the mobility of nodes by characterizing the link lifetime.
- 2) The presented road weight evaluation (RWE) scheme based on the QoF is employed to evaluate each road segment using the built backbone link. The evaluation results can provide quantitative analysis for selecting the best routing path.
- 3) The city map is divided into a series of grid zones to deal with the big network scale. The packet can be forwarded toward the destination by using different transmission strategies based on the position of the destination.

The remainder of this paper is summarized as follows. Section II reviews the related work. Section III presents the assumptions and system model. Section IV gives an overview of our proposed protocol. Two analytical models,

namely, route reliability model and QoF model are presented in Section V and VI, respectively. Section VII gives the RWE scheme. Section VIII proposes the routing algorithm. Performance evaluation is discussed in Section IX, followed by the conclusion in Section X.

II. RELATED WORK

Geographic routing is a promising approach for data transmission in VANETs because its protocols can work just by using local knowledge of the network topology without maintaining or building the route information among nodes. The well-known protocol is GPSR [23], which combines the features of greedy forwarding with perimeter routing to forward the packet. As an improvement of GPSR, MM-GPSR [12] makes the selection of the next hop by considering the cumulative communication duration in greedy forwarding and selects the node with the minimum angle as the optimal relay node in perimeter forwarding. However, both of these are prone to endure routing loops because of the presence of intersections in urban VANETs.

Due to dynamic topology changing, path loss, fading and interference in VANETs, reflecting the link quality is quite challenging. ETX is probably the most well-known metric to measure the forwarding quality of the link between two nodes. Actually, it has been enhanced by recent work for routing metric design in VANETs. LLA [21] introduces a special metric of link cost that combines the packet delivery ratio and the level of link stability to reflect the link performance. Based on the metric, an any-path route between a source node and a destination node can be built. HLAR [20] presents a new hybrid location-based protocol, which makes the combination of a modified AODV protocol and a greedy-forwarding protocol. The AODV augmented with the ETX metric is used to discover the best route. Although these protocols consider the link quality to some extent by exploring the ETX, they still fail to reflect the effect of relative link positions on the network performance.

Intersection-based routing protocols are more effective and stable in VANETs. Intersection-based and traffic-aware routing (IDTAR) [24] dynamically selects the next intersection by considering the remaining distance from each candidate intersection to the destination as well as the density. However, the road segment with high density is preferred for packet forwarding in IDTAR, where the channel contention is intensified in case of heavy data flows. Due to the dynamic topology changes, connectivity is a key indicator of link availability, which has been utilized by several researchers to devise a routing scheme [14], [15], [25]. SDCR [14] proposes a connectivity-aware protocol, where the connectivity is calculated based on the distribution and number of nodes with road segments. The inter-level transmission is conducted based on the connectivity of road segments. EGSR [15] employs an ant-based algorithm to propose a traffic-aware position-based routing scheme. In EGSR, the weight of each road segment is calculated based on the

network connectivity of that segment. The complete routing path between a source node and a destination node with the minimum total weight is determined as the best route. However, SDCR [14] and EGSR [15] cannot fully reflect the channel environment and allow for load balancing. The transmission delay is leveraged as the important metric of routing selection in MADR [17] and stable CDS-based routing protocol (SCRIP) [26]. Before forwarding the data, they determine a complete end-to-end route with the lowest delay. Without considering the variation of network topology, sub-optimal routing decisions may be made. In order to deal with this issue, real-time intersection-based segment-aware routing (RTISAR) [6] and lightweight intersection-based traffic-aware routing (LITAR) [27] make dynamic routing selection for data transmission. RTISAR [6] aims to find the best route for data forwarding by taking into account of traffic segment status. The traffic segment status is measured according to connectivity, density, load as well as distance toward the destination. LITAR [27] devises a scheme that forwards data based on three metrics, i.e., directional node density, road network connectivity, and distance toward the destination. Two algorithms are proposed to reduce the overhead brought by the real-time traffic and network status measurement mechanism. Different from these intersection-based protocols above, the novelty of reliable path selection and packet forwarding routing protocol (RPSPF) [28] lies in the fact that it determines multiple roads to forward data at intersections. Many efforts have been devoted to exploiting vehicular trajectories for data forwarding in VANETs. By exploiting the characteristics of bus networks, [29] presents the bus trajectory-based street-centric (BTSC) routing protocol, where buses are employed as relay nodes to deliver data. The routing path with high density of buses and low probability of transmission direction deviating from the routing path is selected to route the data. In [16], depending on the trajectory information of vehicles in a specified vehicular network, a vehicle encounter graph is constructed to predict vehicle encounter events. With this encounter graph, the data forwarding process can be optimized for minimal delay under a delivery ratio constraint. However, [16] is mainly applicable in light traffic environments.

Due to a lack of pervious works on the development of reliable routing in VANETs, this paper explores the effect of link positions on the network performance with backbone nodes. The main symbols we used are listed in Table 1 for reference.

III. ASSUMPTIONS AND SYSTEM MODEL

A. ASSUMPTIONS

Each vehicle is equipped with a digital map and can get its position and speed by the GPS. The geographical position of the destination vehicle can be obtained by using a location service. These assumptions have been adopted widely in previous studies, e.g., [18] and [30].

TABLE 1. Summary of main symbols.

Symbol	Description
R	Average vehicle reception range
p_{suc}	The probability of a sender to send a packet successfully
$f_V(v)$	The probability distribution function of vehicle's speed
v_{min}	The minimum value of vehicle's speed
v_{max}	The maximum value of vehicle's speed
v_r	The relative speed between two vehicles
$f_{V_r}(v_r)$	The probability distribution function of v_r
$p_{s_i s_j}$	The transition probability of state S_i being translated into state S_j
\mathbf{P}	Distance transition matrix
T_{link}	Average connection time between two vehicles
$r(L(v_0, v_n))$	Link reliability between vehicle v_0 and vehicle v_n
K	The number of transmissions needed for successfully forwarding a packet between two vehicles
Y_n	The number of end-to-end attempts needed for the packet to be forwarded toward the destination
p_{ij}	The successful packet delivery ratio between vehicle i and vehicle j
q_n	Link quality of forwarding between vehicle v_0 and vehicle v_n
$E[q_n]$	Average value of q_n
t_{cross}	The time the vehicle crosses the intersection zone
$s_{optimal}$	Optimal next hop
$Q(P_i)$	Quality of forwarding of path P_i
$R(P_i)$	Link reliability of path P_i
$q(r_{ij})$	Quality of forwarding of road r_{ij}
$r(r_{ij})$	Link reliability of road r_{ij}
$c_{optimal}$	Optimal intersection

B. CHANNEL FADING MODEL

The Nakagami-m model is used to describe the fading of radio wave propagation, where the probability density function (PDF) of received signal power x is given by [31]: $P_z(x) = \left(\frac{m}{P_r}\right)^m \frac{x^{m-1}}{\Gamma(m)} e^{-\frac{mx}{P_r}}$, for $x \geq 0$. $\Gamma(\cdot)$ is the Gamma function; $P_r = \frac{P_t \Omega}{r^\alpha}$ is the average received power; P_t is the transmission power; r is the distance in meters; α is the path-loss exponent; $\Omega = G_t G_r \left(\frac{C}{4\pi f_c}\right)^2$; C is the light speed; $f_c = 5.9$ GHZ is the carrier frequency; G_t and G_r are the transmitter's and receiver's antenna gains, respectively; and m is the fading factor. Based on the Nakagami-m model, the cumulative distribution function (CDF) of the communication range of vehicles when the received power is greater than one specific threshold P_{th} is expressed as: $F_R(r) = 1 - \int_{P_{th}}^{\infty} P_z(x) dx = 1 - \frac{1}{\Gamma(m)} \sum_{i=0}^{m-1} \frac{(m-1)!}{(m-1-i)!} \left(\frac{mP_{th}}{P_r}\right)^{m-1-i} e^{-\frac{mP_{th}}{P_r}}$. Thus, the average vehicle reception range with channel fading considered denoted by R is derived as:

$$R = \int_0^{\infty} (1 - F_R(r)) dr = \frac{1}{\alpha \Gamma(m)} \sum_{i=0}^{m-1} \frac{(m-1)!}{(m-1-i)!} \left(\frac{mP_{th}}{P_r}\right)^{m-1-i} \times \Gamma(m-1-i + \frac{1}{\alpha}) \left(\frac{mP_{th}}{P_r \Omega}\right)^{-\frac{1}{\alpha}}. \quad (1)$$

C. CHANNEL CONTENTION MODEL

A contention-based access scheme is employed in the media access control (MAC) layer to resolve vehicular

channel contentions. Specifically, the request to send/clear to send (RTS/CTS) mechanism is adopted to eliminate hidden terminals and the 802.11 IEEE DCF is used for the MAC layer scheduling. We denote W as the minimum contention window size in the exponential backoff. Then, the average transmission probability of a successful data transmission can be given denoted as: $\delta = \frac{2}{W+2}$ [32], by which the probability of a sender to successfully transmit a packet is derived as:

$$p_{suc} = (1 - \delta)^N, \quad (2)$$

where N indicates the number of the sender's neighbors.

D. VEHICULAR TRAFFIC MODEL

Referring to [33], we assume that the speed of the vehicles is uniformly distributed in an interval (v_{min}, v_{max}) where v_{min} and v_{max} indicate the minimum speed and maximum speed of vehicles. The PDF of the speed is expressed as:

$$f_V(v) = \frac{1}{v_{max} - v_{min}}, \quad v_{min} \leq v \leq v_{max}. \quad (3)$$

IV. OVERVIEW OF OUR PROPOSED ROUTING PROTOCOL

Our proposed QFRG protocol aims to find an optimal routing path composed of a series of road segments between a source node and a destination node. In order to achieve this goal, two novel metrics of link reliability and QoF are utilized, where link reliability is leveraged to measure the availability of a link with the consideration of the mobility of vehicles and QoF is devised by considering the transmission cost, packet delivery ratio as well as relative link positions. With the assistance of QoF, an RWE scheme is developed to evaluate each road segment via the selected backbone nodes at intersections and within road segments. The city map is divided into a series of small GZs to deal with the large network scale. Based on the position of the destination, the packet can be forwarded toward the destination by selecting the GZ one by one. In each GZ, the packet is delivered along the routing path which can guarantee the QoF while satisfying the link reliability. In summary, the main components of our proposed routing protocol include: 1) link reliability, 2) quality of forwarding, 3) road weight evaluation scheme, 4) optimized routing path selection algorithm. The framework of our proposed routing protocol is illustrated in Fig. 3.

V. LINK RELIABILITY

Due to the mobility of nodes in VANETs, link partitions frequent happen, which will disturb data transmission and lead to transmission failure [34], [35]. Thus, link reliability plays an important role in improving the network performance [36]. In this section, we give single-hop/one-hop and multi-hop link reliability models, respectively.

A. ONE-HOP LINK RELIABILITY MODEL

In this subsection, we use the average link connection time between two nodes to reflect one-hop link reliability.

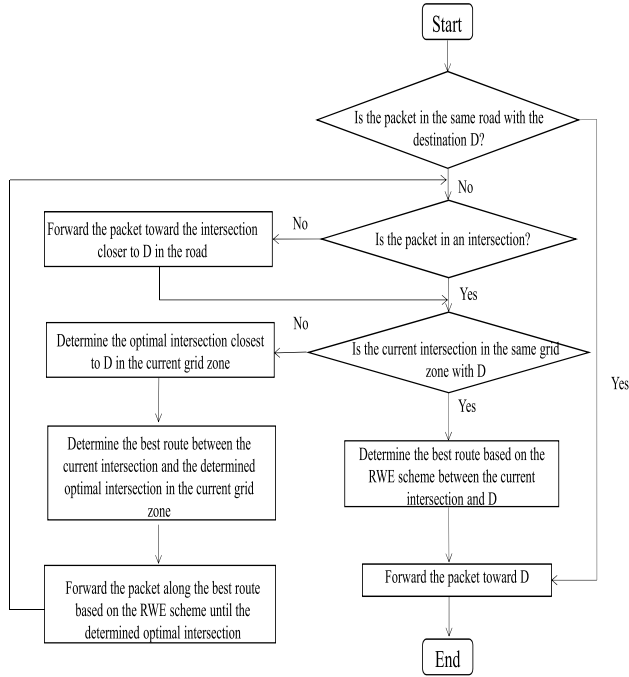


FIGURE 3. The framework of the proposed routing protocol.

Consider two adjacent nodes A and B. If they are moving in the same direction, their relative speed v_r lies in the interval $(-v_m, v_m)$, where $v_m = v_{\max} - v_{\min}$. Based on (3), the PDF of v_r is derived as:

$$f_{v_r}(v_r) = \begin{cases} \frac{v_{\max} - v_{\min} + v_r}{(v_{\max} - v_{\min})^2}, & -v_m \leq v_r \leq v_m \\ \frac{v_{\max} - v_{\min} - v_r}{(v_{\max} - v_{\min})^2}, & 0 \leq v_r \leq v_m. \end{cases}$$

If they are moving in the opposite directions, their relative speed v_r lies in the interval $(2v_{\min}, 2v_{\max})$. In this case, according to (3), the PDF of v_r is formulated as:

$$f_{v_r}(v_r) = \begin{cases} \frac{v_r - 2v_{\min}}{(v_{\max} - v_{\min})^2}, & 2v_{\min} \leq v_r \leq v_{\min} + v_{\max} \\ \frac{2v_{\max} - v_r}{(v_{\max} - v_{\min})^2}, & v_{\min} + v_{\max} \leq v_r \leq 2v_{\max}. \end{cases}$$

In order to view the mobility behavior of one vehicle at the microscopic level, we divide the time into small time steps with the same interval length τ . Let X_m represent the inter-vehicle distance between A and B after m time steps. Then, $X_m = X_{m-1} + v_r \tau$. For simplicity, it is assumed that $\tau = 1$. Thus, we have $X_m = X_{m-1} + v_r$. Similar to [33], the link connection time is defined as:

$$T_{link} = \sup_{m>0} \{m \cdot \tau : X_i \leq R, 1 \leq i \leq m\}. \quad (4)$$

We partition the transmission range R into h equal intervals with the same width $\varepsilon = \frac{R}{h}$. State S_i ($i = 1, 2, \dots, h$) indicates the inter-vehicle distance between two nodes which lies in the small zone $[(i-1)\varepsilon, i\varepsilon]$. S_{h+1} is the absorbing state, representing the terminal state for the entire communication

period, where the inter-vehicle distance is greater than R . Note that S_0 indicates the initial inter-vehicle distance. Then, we can get the conditional distance transition probability that the inter-vehicle distance is changed from current state S_i to next state S_j as [33]:

$$\begin{aligned} p_{s_i s_j} &= \text{prob}\{X_m \in S_j / X_{m-1} \in S_i\} \\ &= \frac{\text{prob}\{(j-1)\tau \leq X_m \leq j\tau \cap (i-1)\tau \leq X_{m-1} \leq i\tau\}}{\text{prob}\{(i-1)\tau \leq X_{m-1} \leq i\tau\}} \\ &= \frac{\int_{(i-1)\varepsilon}^{i\varepsilon} \int_{(j-1)\varepsilon}^{j\varepsilon} f_{X_i/X_{i-1}}(x_i/x_{i-1}) f_{X_{i-1}}(x_{i-1}) dx_{i-1} dx_i}{\int_{(i-1)\varepsilon}^{i\varepsilon} f_{X_{i-1}}(x_{i-1}) dx_{i-1}}, \quad (5) \end{aligned}$$

where $f_{X_i/X_{i-1}}(x_i/x_{i-1}) f_{X_{i-1}}(x_{i-1})$ is denoted as the conditional PDF of X_m given X_{m-1} which can be calculated as: $\int_{(j-1)\varepsilon}^{j\varepsilon} f_{X_i/X_{i-1}}(x_i/x_{i-1}) f_{X_{i-1}}(x_{i-1}) dx_{i-1} = f_{v_r}(v_r)$, and $f_{X_{i-1}}(x_{i-1}) dx_{i-1}$ is the marginal PDF of X_{m-1} which can be derived as: $f_{X_{i-1}}(x_{i-1}) dx_{i-1} = \frac{1}{\varepsilon}$ when ε is set to a sufficiently small value. We assume that $p_{s_i s_j} = 1$, $i, j = n+1$ and $p_{s_i s_i} = 0$, $i = n+1, j \neq n+1$. Furthermore, $p_{s_i s_{n+1}} = 1 - \sum_{j=1}^n p_{s_i s_j}$.

Let π_i^0 be the probability that inter-vehicle distance is in state S_i when the link is initialized [37] and π_i^m indicate the probability of the inter-vehicle distance being in state S_i after m time steps. Define Π^0 as the initial probability vector whose i th element is π_i^0 , Π^m as the vector whose i th element is π_i^m , and \mathbf{P} as the distance transition matrix whose element is $p_{s_i s_j}$. Based on the Chapman-Kolmogorov equation, $\Pi^m = \Pi^0 \mathbf{P}^m$. The probability mass function (PMF) of the link connection time can be expressed as:

$$\begin{aligned} \Pr\{T_{link} = k\tau\} &= \Pr\{t_{ij} \leq k\tau\} - \Pr\{t_{ij} \leq (k-1)\tau\} \\ &= [\prod_{h+1}^0 \mathbf{P}^k]_{h+1} - [\prod_{h+1}^0 \mathbf{P}^{k-1}]_{h+1}. \quad (6) \end{aligned}$$

Further, the average link connection time is computed as:

$$T_{link} = \sum_{k=1}^{\infty} k\tau \Pr\{T_{link} = k\tau\}. \quad (7)$$

B. MULTI-HOP LINK RELIABILITY MODEL

The multi-hop link reliability is defined as the minimum connection time value among all one-hop links along the routing path. For a route $L(v_0, v_n)$ between source node v_0 and destination v_n which consists of n one-hop links as shown in Fig. 4, its link reliability is expressed as follows:

$$r(L(v_0, v_n)) = \min_{i \in \{1, 2, \dots, n\}} \{t_{(i-1)i}\}, \quad (8)$$

where $t_{(i-1)i}$ indicates the link connection time which can be calculated based on (7).

VI. QUALITY OF FORWARDING (QoF)

The routing metric plays a key role in determining the optimal route.

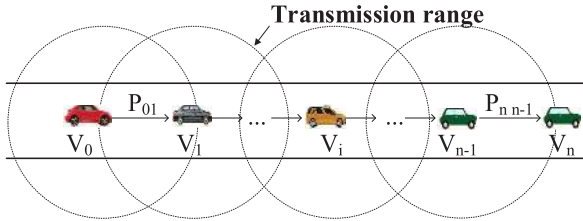


FIGURE 4. Example of a path with different links.

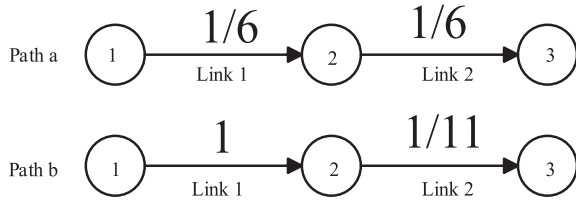


FIGURE 5. Example of two paths with the same ETX.

A. POSITION CORRELATION

ETX is widely utilized to estimate the link quality between two nodes and is based on the assumption that the link layer allows an infinite number of transmissions at each link, i.e., the link layer never drop a packet. The ETX value along a path is estimated by the aggregate of the ETX values of all the links along this path. Although simplifying the calculation of the expected number of transmissions is needed for successful packet delivery along the path, the relative positions of all the links are ignored. Actually, two paths with the same ETX value may use different network resources and incur different network costs. This phenomenon reflects the effect of relative link positions on the network performance. Take a simplified example shown in Fig. 5 to describe this phenomenon we call position correlation. Two paths exist with the same ETX consisting of two links between node 1 and 3. The number appended to each link indicates the probability of a packet to successfully pass the link. The two paths have the common ETX value, that is, 12, i.e., $ETX_{path a} = 6 + 6 = 12$ and $ETX_{path b} = 1 + 11 = 12$. However, both paths actually have different path reliabilities, causing different transmission costs and data packet delivery ratios. Assume the link layer has at most two transmissions per packet. For *path a*, the probability of a packet to pass the link 1 and link 2 is $\frac{1}{6} + (1 - \frac{1}{6}) \cdot \frac{1}{6} = \frac{11}{36}$, respectively. Thus, the probability that a packet successfully passes *path a* is $\frac{11}{36} \times \frac{11}{36} = \frac{121}{1296}$. Similarly, the probability of a packet to successfully traverse *path b* is $\frac{21}{121}$. Apparently, *path b* performs poorly in the reliability for packet forwarding along the path compared with *path a*. This result will be similar even through a higher number of transmissions is considered. Therefore, it can be concluded that ETX fails to account for the transmission cost and path reliability.

B. QoF MODELING

The phenomenon of position correlation motivates us to design one new routing metric QoF on a basis of ETX by

exploring the effect of relative link positions on the network performance. There are $n + 1$ vehicles, i.e., $v_0, v_1, v_2, \dots, v_n$ along a road segment as shown in Fig. 4. They form an n -link connected path, in which vehicles can communicate with each other by wireless communication. The source vehicle v_0 has a packet toward the destination vehicle v_n , and it sends the packet by initiating an end-to-end attempt. The packet will first be forwarded to vehicle v_1 by vehicle v_0 . Upon reception of this packet, vehicle v_1 will continue to forward the packet to vehicle v_2 . The process will be repeated until the packet is received by vehicle v_n . The number of maximum transmissions for a vehicle to forward the packet to an adjacent vehicle is denoted by K . Once the transmission fails, a new transmission attempt will be triggered until the transmission number exceeds the maximum limitation.

In order to realize a successful packet transmission between vehicle v_0 and vehicle v_n , several end-to-end attempts may be needed. For each end-to-end attempt, there is a cost, namely, the number of link level transmissions during the attempt. With the aim to measure the network performance, we defined the QoF as the sum of the costs incurred by all end-to-end attempts for a packet to be forwarded toward vehicle v_n from vehicle v_0 . Next, we discuss how to model the QoF.

Denote Y_n as a random variable to indicate the number of end-to-end attempts needed for a packet to be forwarded toward the destination along a multi-hop path. Denote M_l , $l \subseteq 0, 1, \dots, n$, as the number of consecutive hops that are successfully passed along the path from vehicle v_0 in the l th end-to-end attempt. If the packet sent from vehicle v_0 fails to reach vehicle v_1 , then $M_l = 0$; if the packet can be received by vehicle v_n , then $M_l = n$. In case $M_l < n$, the $(l + 1)$ th end-to-end attempt begins. Denote $H_{l,j}$ as the retransmission number required for a packet to be delivered from v_j to v_{j+1} in the l th attempt. If $H_{l,j} < K$, the packet is successfully passed through the link between vehicle v_j to v_{j+1} ; for $H_{l,j} = K$, the packet fails to reach vehicle v_{j+1} from vehicle v_j , then a new end-to-end attempt will be triggered at vehicle v_0 . Denote q_n as a random variable to indicate the sum of all the costs incurred by all end-to-end attempts for a packet to be forwarded toward vehicle v_n from vehicle v_0 , then the QoF of the path can be expressed as [38]:

$$q_n = \sum_{i=1}^{Y_n} \left(\left[\sum_{j=0}^{M_l-1} H_{l,j} \right] + K \Phi(l < Y_n) \right), \quad (9)$$

where $\Phi(l < Y_n)$ equals to 1 when $l < Y_n$ and 0 otherwise.

Based on (9), the average value of q_n is derived as [38]:

$$E[q_n] = \left(K + \sum_{j=0}^{n-2} E[H_j | H_j < K] P[M > j | M < n] \right) \times E[Y_n - 1] + \sum_{j=0}^{n-1} E[H_j | H_j < K], \quad (10)$$

where variables $M_i, H_{i,j}$ are simply represented by M and H_j , respectively.

Denote χ_i as the probability of the packet not being dropped on the link $l(v_i, v_j)$. Then, χ_i can be expressed as: $\chi_i = 1 - (1 - p_{ij})^K$, where p_{ij} indicates the successful packet delivery ratio between node i and j calculated using (2). Let $\rho_i = \prod_{m=1}^i \chi_m$, then $p[M > i] = \prod_{m=1}^{i+1} \chi_m = \rho_{i+1}$. In particular, $p[M \geq n] = \rho_n$. In order to calculate (10), three lemmas are given.

Lemma 1: The expected number of consecutive hops along a path for transmitting a packet toward the destination from the source node in case of an unsuccessful transmission is:

$$P[M > j | M < n] = \frac{\rho_{j+1} - \rho_n}{1 - \rho_n}. \quad (11)$$

Proof: Conditioned on $M < n$, the probability of $M > j$ to occur is:

$$\begin{aligned} P[M > j | M < n] &= \frac{P[j < M < n]}{P[M < n]} \\ &= \frac{P[M > j] - P[M \geq n]}{1 - P[M \geq n]} \\ &= \frac{\rho_{j+1} - \rho_n}{1 - \rho_n}. \end{aligned} \quad (12)$$

□

Lemma 2: The expected number of end-to-end attempts needed for successful delivery of a packet to the destination from the source node is:

$$E[Y_n - 1] = \frac{1}{\rho_n} - 1. \quad (13)$$

Proof: According to the definition of Y_n , it is known that when $Y_n = l$, $l - 1$ end-to-end attempts fail before the l th end-to-end attempt succeeds. Thus, Y_n follows a geometric distribution with parameter ρ_n . In this case, we have:

$$E[Y_n - 1] = \frac{1}{\rho_n} - 1. \quad (14)$$

□

Lemma 3: The expected number of transmissions needed on a general link for a successful packet transmission between two adjacent nodes is:

$$E[H_j | H_j < K] = \sum_{j=1}^K j \frac{(1-p)^{j-1} p}{1 - (1-p)^{K+1}}, \quad (15)$$

where p represents the successful packet delivery ratio of this link calculated by (2).

Proof: One successful data transmission between two adjacent nodes means that the needed number of transmissions does not exceed the transmission limitation K . In this case, the expected number of transmissions can be given by:

$$E[H_j | H_j < K] = \sum_{j=1}^K j P(H_i = j | H_i \leq K)$$

$$\begin{aligned} &= \sum_{j=1}^K j \frac{P(H_i = j \cap H_i \leq K)}{P(H_i \leq K)} \\ &= \frac{P(H_i = j)}{1 - P(H_i \leq K)} \\ &= \frac{(1-p)^{j-1} p}{1 - (1-p)^{K+1}}. \end{aligned} \quad (16)$$

□

By using **Lemma 1**, **2** and **3**, (10) can be calculated.

VII. ROAD WEIGHT EVALUATION SCHEME

In order to perform specific actions, some nodes at intersections and within road segments are selected as intersection backbone nodes (IBNs) and road segment backbone nodes (RBNs), respectively. With IBNs and RBNs, we can build one backbone link along each road segment for data transmission, by which the channel contention can be reduced [39], [40]. In order to determine the IBNs and RBNs, two corresponding selection criteria are proposed. After a node is selected as the IBN based on the IBN selection scheme (described later), it will execute a distributed RWE procedure along the built backbone link consisting of a series of RBNs within each adjacent road segment to collect the corresponding topology information and link information. Based on these, the road weight can be calculated with the assistance of the QoF routing metric.

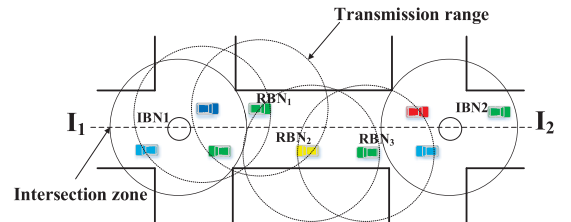


FIGURE 6. Example of RBN selection.

To illustrate the RWE scheme, take a road segment with two intersections I_1 and I_2 as shown in Fig. 6. Once the IBN in intersection I_1 , say IBN1, is determined, it will select one one-hop neighbor node as the RBN. By periodically exchanging beacons with the neighbors, each node can construct its neighboring list where the information (e.g. position and speed) of its neighbors are stored. With these data collected from neighbors, RBN1 is preferred by IBN1 based on the RBN selection scheme (described later). Then, similarly, RBN1 continues to choose RBN2 as the next RBN. This mechanism is repeated till the entire road segment is covered. Finally, one backbone link which consists of two IBNs and a series of RBNs is built in the road segment, e.g., $IBN1 \rightarrow RBN1 \rightarrow RBN2 \rightarrow RBN3 \rightarrow IBN2$, where IBN2 is the intersection backbone node in I_2 . Once the backbone link is built, IBN1 can trigger the RWE scheme by transmitting a unicast road evaluation packet (REP) to I_2 . The format of REP is illustrated in Fig. 7, where *Originator* denotes the node located in an intersection generating

Originator	Intersection _{from}	Intersection _{to}
Timestamp	QoF	Link reliability
Options		

FIGURE 7. Format of REP.

the REP; *Timestamp* denotes the generation time of the REP; *Intersection_{from}* denotes the intersection in which the originator is located; *Intersection_{to}* denotes the intersection towards which the REP will be sent; *QoF* denotes the forwarding quality of the backbone link; *Link reliability* denotes the connection time of the backbone link; *Options* denotes additional routing information, e.g., average density, average speed and hop count. During the process of delivering the REP, the traffic information (e.g., density) and link information (e.g., packet delivery ratio) can be collected [41]. When REP arrives in I_2 , IBN2 is responsible for calculating this road segment weight related to the QoF using (10) based on the collected information. Similar to [41], the calculation result can be sent to the location where the RWE is triggered, i.e., IBN1. In order to reduce the overheads induced by periodic beacons, the frequency of beacons is adjusted to adapt to the varying traffic density. If the network is dense but the network topology is relatively stable, the frequency of beacons is reduced to lower channel congestion; if the density is sparse but the topology is ever-changing, the frequency of beacons can be increased to improve packet delivery ratio. Besides, the available lifetime of the built backbone link can be calculated based on (8). In order to reduce the generated overheads of control packets, the RWE scheme is triggered before the lifetime of the backbone expires.

A. IBN CREATION

1) IBN SELECTION CRITERION

Each IBN is responsible for collecting up-to-date traffic and channel status information, by which each road segment weight can be calculated. Due to the mobility of nodes, the node which stays longer at the intersection zone is the preferred IBN to avoid the frequent changes. The estimated time t_{cross} for one node to cross the intersection zone can be calculated as: $t_{cross} = \frac{d}{v}$, where d indicates the distance needed to move for the node before leaving the intersection zone and v is its current speed.

2) IBN SELECTION PROCEDURE

The IBN selection procedure includes four statuses, and the transition diagram is shown in Fig. 8. Each node will change its status to *monitor* from *sleep* when it enters the intersection zone from one road segment for the first time. Then, it keeps monitoring the status of the specified IBN in the intersection zone. If not receiving any message from one IBN within a predefined period t_p , it means that the node has entered an empty intersection zone. In this case, the node appoints itself as the IBN by changing its status to *spread*. When more than one node enter the empty intersection zone, each node

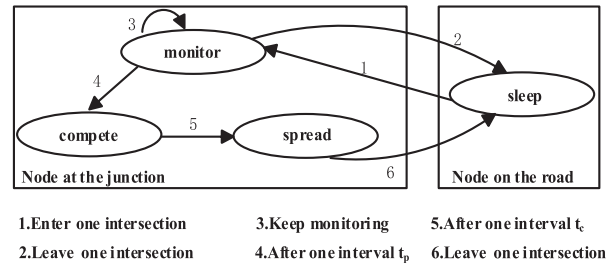


FIGURE 8. Status transitions of nodes.

changes its status to *compete* to compete for the new IBN by setting a countdown timer t_c . Note that the longer the time it stays at the intersection zone, the shorter the countdown timer is assigned. The node whose timer first expires should declare itself to be the new IBN and enter the *spread* state. Receiving the declaration message, all other competitors will cancel their timer at that time and return to the *monitor* status. Periodically, an IBN in the *spread* status should broadcast its existence to its neighbors. When an IBN is about to leave the intersection zone, it should look for a successor that will stay longer at the intersection zone to take over the weight information of road segments in the given zone. After that, the selected successor enters the *spread* state while the previous IBN changes its status to *sleep*.

B. RBN CREATION

In VANETs, the high mobility of vehicles easily leads to link disconnection and interruption of ongoing data transmission. Link connection time is considered an effective metric to estimate the link availability among vehicles. Moreover, the inter-vehicle distance between a sender node and a receiver node impacts the number of hops needed for successful data delivery along a complete path, i.e., the greater the inter-vehicle distance, the lower the number of hops. To deal with the mobility of nodes and reduce the number of hops, we make the selection of RBN by considering both the link connection time and the per-hop coverage distance simultaneously.

Assume a sender node s has k neighbors, forming a set $N(s) = \{s_1, s_2, \dots, s_k\}$. Denote $d(s, i)$ as the inter-vehicle distance between s and its neighbor i . Let t_{si} represent the average link connection time between s and i which can be calculated by (7). Then, the optimal relay node $s_{optimal}$ is selected based on the following criterion:

$$s_{optimal} = \arg \max_{i \in N(s)} d(s, i), \quad \text{subject to } t_{si} > T_{th}, \quad (17)$$

where T_{th} indicates the specified delay threshold determined by the average time for successfully completing a data transmission between two nodes [42].

VIII. OPTIMIZED ROUTING PATH SELECTION ALGORITHM

Due to the considerable size of modern cities, it is extremely difficult to have a global knowledge of the entire city

network topology. To handle this issue, we divide the road map into a series of grid zones (GZs), the size of which is set to 3*3 blocks. When the destination node is far from the source node, the packet can be forwarded toward the destination node by dynamically selecting the GZ one by one. Each GZ can be regarded as a subset of the entire topology. The backbone node IBN_i at intersection i in its GZ periodically disseminates the updated road weight information to adjacent road segments. This way, it can have a global knowledge of the GZ. At first, each IBN in the GZ triggers the RWE scheme to get the weight information of adjacent connected road segments. Then, they need to exchange the weight information with other IBNs. Note that if no message is received from one adjacent IBN during a predetermined period, the road segment between them is supposed to be disconnected and assigned a big weight. After exchanging weight information, each IBN can have a view of the GZ's topology. When a source node S wants to send data packets to a destination node D , it first forwards the packets to the closest IBN. Upon receiving the packets, the IBN checks whether D is in its routing table. Based on the result, there are two possible transmission strategies.

A. DESTINATION NODE IS IN THE ROUTING TABLE

This case means the destination is in the same GZ as the current IBN. Assume there exist M available routes between S and D . Each given route $P_i (i = 1, 2, \dots, M)$, consists of k_i road segments $r_{ij} (j = 1, 2, \dots, k_i)$. Denote $q(r_{ij})$, $r(r_{ij})$ as the QoF and reliability of road segment r_{ij} , respectively. Then, the QoF of the route P_i is given by:

$$Q(P_i) = \sum_{j=1}^{k_i} q(r_{ij}), \quad (18)$$

and the reliability of the route P_i is written as:

$$R(P_i) = \min_{j \in \{1, 2, \dots, k_i\}} r(r_{ij}). \quad (19)$$

In this situation, the issue of finding the optimal route between the source node and the destination node can be formulated as one optimization problem, of which the objective function is expressed as:

$$\begin{aligned} \min_{i \in \{1, 2, \dots, M\}} Q(P_i) \\ \text{subject to } R(P_i) > \varphi_r, \end{aligned} \quad (20)$$

where φ_r indicates the reliability threshold.

B. DESTINATION NODE IS NOT IN THE ROUTING TABLE

This case means that the destination is beyond the GZ where the current IBN is located. In this case, the routing path between S and D is divided into two parts: the first sub-routing path between S and $c_{optimal}$, and the second sub-routing path between $c_{optimal}$ and D . Here, $c_{optimal}$ indicates the optimized intersection in GZ which is the closest one to the destination. Assume there exist N available IBNs in this GZ. Define $d(c_k, D)$ as the distance from each IBN

denoted by $c_k (k = 1, 2, \dots, N)$ to the destination. Then the optimized intersection $c_{optimal}$ is selected according to the following criterion:

$$c_{optimal} = \operatorname{argmin}_{k \in N} d(c_k, D). \quad (21)$$

If there are data packets to be sent, the first optimized sub-routing path between S and $c_{optimal}$ is the first one obtained based on (20). Then these data packets will be forwarded along the backbone link within the sub-routing path. Once they arrive at the intersection $c_{optimal}$, the IBN at the current intersection continues the same procedure illustrated above until the destination is reached. The proposed protocol is illustrated in **Algorithm 1**.

Algorithm 1 QoF-Based Routing in Urban VANETs

Require: S : the packet carrier; D : the destination node; $I_{i,j}$: the road segment with the intersection s_i and s_j along which the packet is moving

- 1: **if** D is within $I_{i,j}$ **then**
- 2: Directly forward the packet to D
- 3: **end if**
- 4: **if** D is within the same GZ with S **then**
- 5: Forward the packet to the IBN located in the closest intersection in the GZ along the transmission direction of the packet and determine the optimized routing path between the IBN and D
- 6: Disseminate the packet along the optimized routing path
- 7: **end if**
- 8: **if** D is beyond the GZ **then**
- 9: Find the intersection $c_{optimal}$ closest to the destination in the GZ
- 10: Determine the optimized sub-routing path between the IBN and $c_{optimal}$
- 11: Disseminate the packet to $c_{optimal}$ along the optimized sub-routing path
- 12: Replace s_i and s_j with $c_{optimal}$ and its neighboring intersection k , respectively and return 1.
- 13: **end if**

IX. PERFORMANCE SIMULATION

In this section, we evaluate the performance of our proposed protocol QFRG under an urban simulation environment by using NS-3 simulator platform. QFRG is compared with three recent routing protocols, namely, MM-GPSR [12], IDTAR [24], RPSPF [28]. For fair comparison, all the routing protocols are enhanced using the carry-and-forward scheme when encountering local optimization, and RPSPF is improved with a real-time traffic information collecting scheme [43].

A. SIMULATION ENVIRONMENT AND PARAMETER SETUP

A simulation of the urban environment of Washington D.C. is used. The simulation map has an area of 7600 m*7600 m.

The initial locations of all the vehicles are randomly located in simulation area. The vehicle movement profile is generated by vehicular ad hoc networks mobility simulator (VANET-MobiSim) along with an intelligent driver model with lane changing (IDM_LC) mobility model [44]. The constant bit rate (CBR) is used to generate the background traffic. Each CBR data is transmitted between a pair of vehicles that are randomly selected. The Nakagami-m model is used to reflect the channel environment [30]. 50 simulation repetitions are implemented to obtain the average result of each simulation scenario with 95% confidence level considered. The important simulation parameters are summarized in Table 2.

TABLE 2. Simulation parameters.

Description	Value
Simulation area	7600 m*7600 m
Number of vehicles	150-600
Vehicular density	2.6-10.4/km ²
Traffic-light interval	1000 ms
Minspeed	8.33 m/s
Maxspeed	22.22 m/s
Beacon message size	15 bytes
Transmission range	250 m
Beacon period	1 s
MAC protocol	802.11p
Packet generation speed	5-50 packets/s
Packet size	512 bytes
Channel capacity	2 Mbps

B. PERFORMANCE METRICS

1) AVERAGE TRANSMISSION DELAY (ATD)

This is the average difference between the time a data packet is generated by an application and the time this packet is received successfully at its destination.

2) PACKET DELIVERY RATIO (PDR)

This is the ratio defined as the total number of packets received at the destination to the total number of packets generated by the source vehicle.

3) COMMUNICATION OVERHEAD (CO)

This is defined as the average control packets generated per road segment

C. SIMULATION RESULTS AND PERFORMANCE ANALYSIS

1) PERFORMANCE ANALYSIS FOR VARYING VEHICULAR DENSITY

The density is expressed in *vehicle/km²* [27], [45]. Fig. 9 shows the performance of all the routing protocols in terms of ATD when the vehicular density (VD) is varying. It is found that with the increase of VD, the ATD of all the protocols is decreased. This is because that in sparse environments, link partitions frequently occur. Thus, the network experiences a high intermittent connectivity. In this case, the carry-and-forward scheme is employed to forward the sent packet until the next hop is found. This causes a large ATD due to the fact that the transmission delay mainly depends on the mobility of

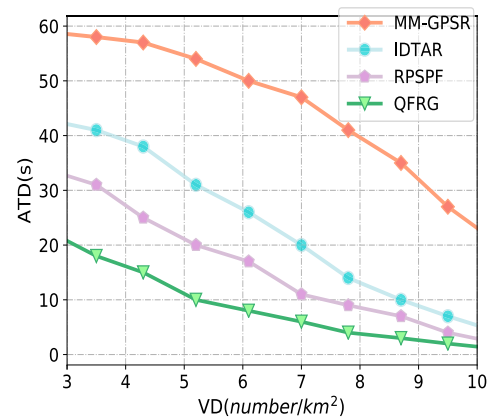


FIGURE 9. Average transmission delay (ATD) vs. Vehicular density (VD).

vehicles for the carry-and-forward scheme. When the VD is increased, the probabilities of vehicles to communicate with each other is enlarged, enhancing the network connectivity. This enables data delivery in multiple-hop wireless transmission manner which leads to the significant reduction with respect to ATD compared to the carry-and-forward scheme. Among all the protocols, MM-GPSR performed the worst ATD. This is attributed to the fact that MM-GPSR forwards the packet mainly based on the greedy scheme. As an enhanced version of GPSR [23], MM-GPSR selects the next hop based on the maximum cumulative communication duration between nodes in greedy forwarding and the minimum angle between nodes in the perimeter forwarding, which has the advantages of dealing with communication instability and redundancy. However, local maximum issue still frequently happens without fully considering the traffic information. In this situation, the largest ATD is exhibited due to the excessive use of the carry-and-forward scheme. Compared to MM-GPSR, road segments are determined progressively to form the optimal route in IDTAR. This protocol selects the next road segment for packet forwarding at intersections by taking into account the remaining distance from the current intersection to the destination and the density. With more traffic information explored, IDTAR outperformed MM-GPSR in terms of ATD. Being an enhancement of IDTAR, RPSPF makes the selection of next road segment by considering the next two immediate intersections dynamically from the current intersection based on the distance toward the destination and the density. Therefore, RPSPF had a slightly better ATD than IDTAR. However, for both IDTAR and RPSPF, road segments with high density are preferred to forward the packet, where the intensified channel contention and signal interference will cause more retransmissions, contributing to the ATD. Compared with the other routing protocols, our proposed protocol QFRG achieved the best performance. QFRG finds the best routing path based on the presented RWE scheme, where the QoF metric is used to give each road segment a suitable weight. With the assistance of QoF, the routing path with good channel quality is selected to forward the packet, which helps reduce ATD. Besides, the

city map is divided into a series of GZs in QFRG to deal with the large network scale. Based on the position of the destination, two different transmission strategies are designed. In case of large network topology, the packet can be forwarded by dynamically selecting the next GZ till the destination, adapting to diverse network scales.

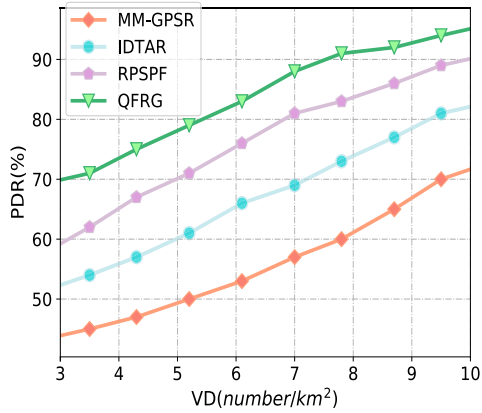


FIGURE 10. Packet delivery ratio (PDR) vs. Vehicular density (VD).

Fig. 10 describes the PDR of all the routing protocols as the function of VD. From this figure, it is noticed that the PDR for all protocols increased as VD increased. The reason for this is that the increase of VD improved the probabilities of vehicles being connected and reduced the number of link partitions. This benefits the reduction of transmission delay incurred by the use of carry-and-forward scheme, lowering the number of dropped packets due to the transmission timeout. Depending only on the geographic information, the road segment with less density is preferred for data forwarding in MM-GPSR. Under this situation, the frequent use of carry-and-forward scheme will greatly contribute to the delivery delay, resulting in the dropping of packets before the packets reach the destination. Therefore, MM-GPSR exhibits the worst PDR. Both IDTAR and RPSPF perform better PDR than MM-GPSR, for the reason that they regard the large volume of vehicular traffic at certain road segments as a positive condition to make the selection of road segments for packet forwarding. RPSPF achieves a slight performance improvement compared to IDTAR. This can be explained that RPSPF makes routing selection by considering multiple intersections and utilizing a reliable data forwarding scheme between two intersections. However, they do not account for the channel environment. When the packets are forwarded along the road segment with high density, the channel contention and signal interference can be greatly intensified. By contrast, QFRG obtains the best performance. From one hand, QFRG finds the best routing path with the consideration of transmission cost and link features. From the other hand, one backbone link is built in each road segment, along which the packets are forwarded. This alleviates the transmission contention in MAC layer. Therefore, QFRG achieves the best PDR compared with the other three routing protocols.

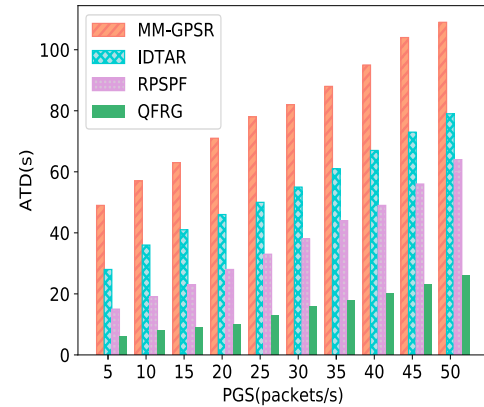


FIGURE 11. Average transmission delay (ATD) vs. Packet generation speed (PGS).

2) PERFORMANCE ANALYSIS FOR VARYING PACKET GENERATION SPEED

Fig. 11 illustrates the ATD of all the routing protocols with respect to varying packet generation speed (PGS). When the PGS is growing, the ATD is increased. This can be explained that with the increase of PGS, more packets are generated in a time interval. This will further result in more collisions and retransmissions, contributing to the ATD. MM-GPSR exhibits the worst ATD. The significant delay is incurred because it is easier to encounter link partitions for MM-GPSR compared with the other protocols. The improvement of IDTAR over MM-GPSR is due to the consideration of vehicular traffic including the distance toward the destination and the density. RPSPF has a slightly better ATD than IDTAR based on two reasons: 1) the first one is that the optimal routing path is determined by taking into multiple intersection which enables the selection of road segments with rich density; 2) the second one is that a reliable link stability scheme is provided to ensure the link with long life-time to implement data forwarding. However, without allowing for load balancing, both of IDTAR and RPSPF will experience severe data congestion in dense environments, escalating the ATD. Different from the other three protocols, QFRG proposes a routing metric QoF by fully considering the link quality and status. Based on the metric, each road segment can be assigned a weight based on the RWE scheme. According to the weight information, the best route can be determined. Using this manner, the ATD can be reduced when the packet is forwarded along the selected optimal routing path.

Fig. 12 shows the PDR by employing different PGS. From the figure, it can be known that the increase of PGS leads to the reduction of PDR. This reason is that due to the mobility and distribution of nodes, link partitions often occur in the VANETs. In this situation, the packet carrier needs to store and carry the packet until the next hop is encountered. Considering the limitation of buffer size, the new coming packets will get dropped when the buffer is full. As a result, with the increase of PGS, the PDR is reduced. Among all the routing protocols, MM-GPSR frequently restores to

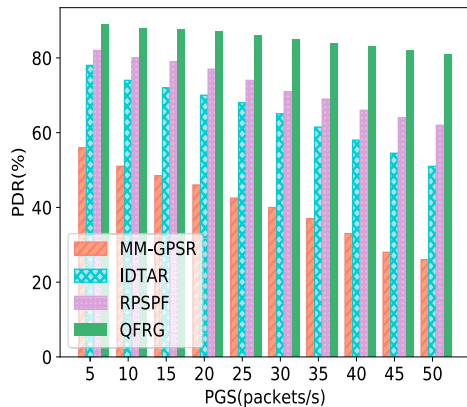


FIGURE 12. Packet delivery ratio (PDR) vs. Packet generation speed (PGS).

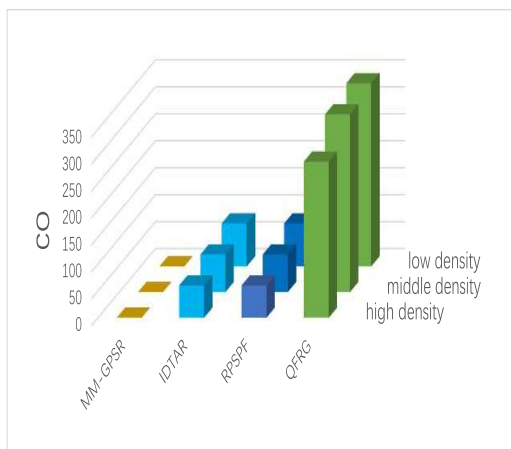


FIGURE 13. Communication overheads.

the carry-and-forward scheme, eventually leading to packet losses. Depending on the existence of vehicular traffic to select the best route for packet forwarding, both IDTAR and RPSPF achieves better PDR than MM-GPSR. Compared to IDTAR, RPSPF performs better in finding road segments with high connectivity and dealing with high mobility of vehicles assisted by the proposed intersection scheme and reliable forwarding strategy. However, the convergence of packets on certain road segments with high density makes IDTAR and RPSPF more transmission failures and retransmissions, reducing the PDR. For QFRG, the routing metric QoF is designed as the guidance of routing selection with the consideration of transmission cost and packet delivery ratio. Based on the metric, the RWE scheme is used to evaluate each road segment by using the real-time traffic information and network status. According to the evaluation, the determined best routing path can enable the improvement of PDR compared with the other routing protocols.

3) COMMUNICATION OVERHEADS

From [41], it is known that beacon packets are main overheads for position-based routing protocols. IDTAR, RPSPF and QFRG incur additional overheads due to the use of control packets for vehicular information collecting along

road segments. However, the frequency of generating such control packets is much lower than the one of generating beacon packets. In the same simulation setting, the average beaconing overheads are same for these protocols. Similar to [41], we mainly focus on the overheads incurred by the use of control packets. We define such communication overheads (CO) as average control packets generated per road segment. The simulation result with respect to communication overheads for these protocol is illustrated in Fig. 13. MM-GPSR is the only protocol which does not generate any CO for the reason that it just depends on the information of neighbors to make routing decisions without triggering any control packets. For IDTAR, RPSPF and QFRG, additional communication overheads are incurred when control packets are used to collect traffic information and link information for data transmission. With the increase in the density, the communication overheads are decreased. This can be explained that when the number of vehicles is increasing, the network topology becomes more stable, which enables the reduction of control packets. Our proposed routing protocol exhibits the greatest communication overheads among all the routing protocols. This is due to the creation of backbone link along the road and the use of road weight packet. However, considering the significant performance improvements in terms of average transmission delay and packet delivery ratio, this small cost can be tolerable.

X. CONCLUSION

In this paper, we proposed a quality of forwarding based reliable geographic routing for urban VANETs. To select the best routing path, two metrics, namely, QoF and link reliability were utilized. The QoF is designed to reflect the channel quality by considering transmission cost, packet delivery ratio and the effect of relative link positions on the network performance, while the link reliability represented the link lifetime characterizing the mobility of the nodes. Road segments can be evaluated based on the RWE scheme, where the backbone link is built to deliver data. Moreover, the city map is divided into a series of small zones. The packet can be forwarded to the destination by selecting the zone one by one. In each zone, the routing path which guarantees the QoF while satisfying the link reliability requirement is used to forward the packet. Simulation results indicate that our proposed protocol outperformed existing schemes in terms of transmission delay and packet delivery ratio.

REFERENCES

- [1] Y. Dai, D. Xu, S. Maharjan, and Y. Zhang, "Joint load balancing and offloading in vehicular edge computing and networks," *IEEE Internet Things J.*, to be published. doi: [10.1109/JIOT.2018.2876298](https://doi.org/10.1109/JIOT.2018.2876298).
- [2] H. Peng, L. Liang, X. Shen, and G. Y. Li, "Vehicular communications: A network layer perspective," *IEEE Trans. Veh. Technol.*, vol. 68, no. 2, pp. 1064–1078, Feb. 2019. doi: [10.1109/TVT.2018.2833427](https://doi.org/10.1109/TVT.2018.2833427).
- [3] Z. Zhou, H. Yu, C. Xu, Y. Zhang, S. Mumtaz, and J. Rodriguez, "Dependable content distribution in D2D-based cooperative vehicular networks: A big data-integrated coalition game approach," *IEEE Trans. Intell. Transp. Syst.*, vol. 19, no. 3, pp. 953–964, Mar. 2018.
- [4] Z. Zhou, C. Gao, C. Xu, Y. Zhang, S. Mumtaz, and J. Rodriguez, "Social big-data-based content dissemination in Internet of vehicles," *IEEE Trans. Ind. Informat.*, vol. 14, no. 2, pp. 768–777, Feb. 2018.

- [5] L. Ma, X. Liu, Q. Pei, and Y. Xiang, "Privacy-preserving reputation management for edge computing enhanced mobile crowdsensing," *IEEE Trans. Services Comput.*, to be published. doi: [10.1109/TSC.2018.2825986](https://doi.org/10.1109/TSC.2018.2825986).
- [6] Y. R. B. Al-Mayouf *et al.*, "Real-time intersection-based segment aware routing algorithm for urban vehicular networks," *IEEE Trans. Intell. Transp. Syst.*, vol. 19, no. 7, pp. 2125–2141, Jul. 2018.
- [7] T. S. J. Darwish, K. A. Bakar, and K. Haseeb, "Reliable intersection-based traffic aware routing protocol for urban areas vehicular ad hoc networks," *IEEE Intell. Transp. Syst. Mag.*, vol. 10, no. 1, pp. 60–73, Jan. 2018.
- [8] L. Liu, C. Chen, T. Qiu, M. Zhang, S. Li, and B. Zhou, "A data dissemination scheme based on clustering and probabilistic broadcasting in VANETs," *Veh. Commun.*, vol. 13, pp. 78–88, Jul. 2018. doi: [10.1016/j.vehcom.2018.05.002](https://doi.org/10.1016/j.vehcom.2018.05.002).
- [9] C. Chen, L. Liu, X. Du, X. Wei, and C. Pei, "Available connectivity analysis under free flow state in VANETs," *EURASIP J. Wireless Commun. Netw.*, vol. 2012, no. 1, pp. 1–19, Dec. 2012.
- [10] M. H. Eiza and Q. Ni, "An evolving graph-based reliable routing scheme for VANETs," *IEEE Trans. Veh. Technol.*, vol. 62, no. 4, pp. 1493–1504, May 2013.
- [11] J. Kang *et al.*, "Blockchain for secure and efficient data sharing in vehicular edge computing and networks," *IEEE Internet Things J.*, to be published. doi: [10.1109/JIOT.2018.2875542](https://doi.org/10.1109/JIOT.2018.2875542).
- [12] X. Yang, M. Li, Z. Qian, and T. Di, "Improvement of GPSR protocol in vehicular ad hoc network," *IEEE Access*, vol. 6, pp. 39515–39524, 2018. doi: [10.1109/ACCESS.2018.2853112](https://doi.org/10.1109/ACCESS.2018.2853112).
- [13] P. K. Sahu, E. H.-K. Wu, J. Sahoo, and M. Gerla, "BAHG: Back-bone-assisted hop greedy routing for VANET's city environments," *IEEE Trans. Intell. Transp. Syst.*, vol. 14, no. 1, pp. 199–213, Mar. 2013.
- [14] X. Zhang, Z. Wang, and X. Jiang, "A realistic spatial-distribution-based connectivity-aware routing protocol in multilevel scenarios of urban VANETs," *IEEE Commun. Lett.*, vol. 22, no. 9, pp. 1906–1909, Sep. 2018. doi: [10.1109/LCOMM.2018.2855195](https://doi.org/10.1109/LCOMM.2018.2855195).
- [15] F. Goudarzi, H. Asgari, and H. S. Al-Rawashidy, "Traffic-aware VANET routing for city environments—A protocol based on ant colony optimization," *IEEE Syst. J.*, vol. 13, no. 1, pp. 571–581, Mar. 2019. doi: [10.1109/JSYST.2018.2806996](https://doi.org/10.1109/JSYST.2018.2806996).
- [16] J. P. Jeong *et al.*, "TPD: Travel prediction-based data forwarding for light-traffic vehicular networks," *Comput. Netw.*, vol. 93, pp. 166–182, Dec. 2015.
- [17] J. He, L. Cai, J. Pan, and P. Cheng, "Delay analysis and routing for two-dimensional VANETs using carry-and-forward mechanism," *IEEE Trans. Mobile Comput.*, vol. 16, no. 7, pp. 1830–1841, Jul. 2017.
- [18] N. Li, J. F. Martínez-Ortega, V. H. Díaz, and J. A. S. Fernandez, "Probability prediction-based reliable and efficient opportunistic routing algorithm for VANETs," *IEEE/ACM Trans. Netw.*, vol. 26, no. 4, pp. 1933–1947, Aug. 2018. doi: [10.1109/TNET.2018.2852220](https://doi.org/10.1109/TNET.2018.2852220).
- [19] J. Wang, Y. Liu, Y. He, W. Dong, and M. Li, "QoF: Towards comprehensive path quality measurement in wireless sensor networks," *IEEE Trans. Parallel Distrib. Syst.*, vol. 25, no. 4, pp. 1003–1013, Apr. 2014.
- [20] M. Al-Rabayah and R. Malaney, "A new scalable hybrid routing protocol for VANETs," *IEEE Trans. Veh. Technol.*, vol. 61, no. 6, pp. 2625–2635, Jul. 2012.
- [21] J. Rak, "LLA: A new anypath routing scheme providing long path lifetime in VANETs," *IEEE Commun. Lett.*, vol. 18, no. 2, pp. 281–284, Feb. 2014.
- [22] M. Radi, B. Dezfouli, K. A. Bakar, A. S. Razak, and M. Lee, "Linkord: Link ordering-based data gathering protocol for wireless sensor networks," *Computing*, vol. 97, no. 3, pp. 205–236, Mar. 2015.
- [23] V. Naumov, R. Baumann, and T. Gross, "An evaluation of inter-vehicle ad hoc networks based on realistic vehicular traces," in *Proc. ACM MobiHoc*, Florence, Italy, May 2006, pp. 108–119.
- [24] A. I. A. Ahmed, A. Gani, S. H. A. Hamid, S. Khan, N. Guizani, and K. Ko, "Intersection-based distance and traffic-aware routing (IDTAR) protocol for smart vehicular communication," in *Proc. IWCMC*, Valencia, Spain, Jun. 2017, pp. 489–493.
- [25] C. Chen, Y. Jin, Q. Pei, and N. Zhang, "A connectivity-aware intersection-based routing in VANETs," *EURASIP J. Wireless Commun. Netw.*, vol. 2014, no. 1, pp. 1–16, 2014.
- [26] M. A. Togou, A. Hafid, and L. Khoukhi, "SCRIP: Stable CDS-based routing protocol for urban vehicular ad hoc networks," *IEEE Trans. Intell. Transp. Syst.*, vol. 17, no. 5, pp. 1298–1307, May 2016.
- [27] T. Darwish and K. A. Bakar, "Lightweight intersection-based traffic aware routing in Urban vehicular networks," *Comput. Commun.*, vol. 87, pp. 60–75, Aug. 2016.
- [28] I. A. Abbasi, A. S. Khan, and S. Ali, "A reliable path selection and packet forwarding routing protocol for vehicular ad hoc networks," *EURASIP J. Wireless Commun. Netw.*, vol. 2018, no. 1, p. 236, Dec. 2018.
- [29] G. Sun, Y. Zhang, D. Liao, H. Yu, X. Du, and M. Guizani, "Bus-trajectory-based street-centric routing for message delivery in urban vehicular ad hoc networks," *IEEE Trans. Veh. Technol.*, vol. 67, no. 8, pp. 7550–7563, Aug. 2018.
- [30] X. M. Zhang, K. H. Chen, X. L. Cao, and D. K. Sung, "A street-centric routing protocol based on microtopology in vehicular ad hoc networks," *IEEE Trans. Veh. Technol.*, vol. 65, no. 7, pp. 5680–5694, Jul. 2016.
- [31] K. A. Hafeez, L. Zhao, B. Ma, and J. W. Mark, "Performance analysis and enhancement of the DSRC for VANET's safety applications," *IEEE Trans. Veh. Technol.*, vol. 62, no. 7, pp. 3069–3083, Sep. 2013.
- [32] T. H. Luan, X. S. Shen, and F. Bai, "Integrity-oriented content transmission in highway vehicular ad hoc networks," in *Proc. IEEE INFOCOM*, Turin, Italy, Apr. 2013, pp. 2562–2570.
- [33] S. Shelly and A. V. Babu, "Modeling and analysis of link duration in vehicular ad hoc networks under different fading channel conditions," *Int. J. Wireless Inf. Netw.*, vol. 22, no. 3, pp. 157–170, Sep. 2015.
- [34] K. Zhang, Y. Mao, S. Leng, Y. He, and Y. Zhang, "Mobile-edge computing for vehicular networks: A promising network paradigm with predictive offloading," *IEEE Veh. Technol. Mag.*, vol. 12, no. 2, pp. 36–44, Jun. 2017.
- [35] J. Du, F. R. Yu, X. Chu, J. Feng, and G. Lu, "Computation offloading and resource allocation in vehicular networks based on dual-side cost minimization," *IEEE Trans. Veh. Technol.*, vol. 68, no. 2, pp. 1079–1092, Feb. 2019. doi: [10.1109/TVT.2018.2883156](https://doi.org/10.1109/TVT.2018.2883156).
- [36] C. Chen, H. Jinna, T. Qiu, M. Atiquzzaman, and Z. Ren, "CVCG: Cooperative V2V-aided transmission scheme based on coalitional game for popular content distribution in vehicular ad-hoc networks," *IEEE Trans. Mobile Comput.*, to be published. doi: [10.1109/TMC.2018.2883312](https://doi.org/10.1109/TMC.2018.2883312).
- [37] Q. Han, Y. Bai, L. Gong, and W. Wu, "Link availability prediction-based reliable routing for mobile ad hoc networks," *IET Commun.*, vol. 5, no. 16, pp. 2291–2300, Nov. 2011.
- [38] G. Jakllari, S. Eidenbenz, N. Hengartner, S. V. Krishnamurthy, and M. Faloutsos, "Link positions matter: A noncommutative routing metric for wireless mesh networks," *IEEE Trans. Mobile Comput.*, vol. 11, no. 1, pp. 61–72, Jan. 2012.
- [39] C. Wu, S. Ohzahata, Y. Ji, and T. Kato, "How to utilize interflow network coding in VANETs: A backbone-based approach," *IEEE Trans. Intell. Transp. Syst.*, vol. 17, no. 8, pp. 2223–2237, Aug. 2016.
- [40] C. Li, Y. Zhang, T. H. Luan, and Y. Fu, "Building transmission backbone for highway vehicular networks: Framework and analysis," *IEEE Trans. Veh. Technol.*, vol. 67, no. 9, pp. 8709–8722, Sep. 2018.
- [41] N. Alsharif, S. Céspedes, and X. S. Shen, "iCAR: Intersection-based connectivity aware routing in vehicular ad hoc networks," in *Proc. IEEE Int. Conf. Commun. (ICC)*, Jun. 2013, pp. 1736–1741.
- [42] X. Li, B.-J. Hu, H. Chen, B. Li, H. Teng, and M. Cui, "Multi-hop delay reduction for safety-related message broadcasting in vehicle-to-vehicle communications," *IET Commun.*, vol. 9, no. 3, pp. 404–411, Feb. 2015.
- [43] M. Jerbi, S. M. Senouci, T. Rasheed, and Y. Ghamri-Doudane, "Towards efficient geographic routing in urban vehicular networks," *IEEE Trans. Veh. Technol.*, vol. 58, no. 9, pp. 5048–5059, Nov. 2009.
- [44] J. Håri, F. Filali, C. Bonnet, and M. Fiore, "VanetMobiSim: Generating realistic mobility patterns for VANETs," in *Proc. ACM SIMUTOOLS*, Los Angeles, USA, Sep. 2006, pp. 96–97.
- [45] T. Darwish and K. A. Bakar, "Traffic density estimation in vehicular ad hoc networks: A review," *Ad Hoc Netw.*, vol. 24, pp. 337–351, Jan. 2015.



LEI LIU (S'17) received the B.Eng. degree in communication engineering from Zhengzhou University, Zhengzhou, China, in 2010, and the M.Sc. degree in communication engineering from Xidian University, Xi'an, China, in 2013, where he is currently pursuing the Ph.D. degree. He has published more than ten journals and conference publications. He is currently a Visiting Ph.D. Student with the Department of informatics, University of Oslo, Norway. His research interests include vehicular

ad hoc networks, intelligent transportation, mobile edge computing and the Internet of Things. He and his co-workers received the Best Paper Award at the ICITE 2016, SmartIoT 2018, and WPMC 2018.



CHEN CHEN (M'09–SM'18) received the B.Eng., M.Sc., and Ph.D. degrees in electrical engineering and computer science (EECS) from Xidian University, Xi'an, China, in 2000, 2006, and 2008, respectively, where he is currently an Associate Professor with the Department of EECS. He was a Visiting Professor of EECS with The University of Tennessee and a Visiting Professor of CS with the University of California. He is also the Director of the Xi'an Key Laboratory of Mobile Edge

Computing and Security and the Intelligent Transportation Research Laboratory, Xidian University. He has authored/co-authored two books and over 80 scientific papers in international journals and conference proceedings. He has contributed to the development of five copyrighted software systems and invented 50 patents. He is also a Senior Member of the China Computer Federation (CCF) and a member of the ACM and the Chinese Institute of Electronics. He serves as the General Chair, the PC Chair, the Workshop Chair, and a TPC Member of a number of conferences.



BIN WANG received the B.Eng., M.Sc., and Ph.D. degrees in electrical engineering and computer science (EECS) from Xidian University, Xi'an, China, in 2003, 2006, and 2011, respectively. Since 2011, he has been with the School of Communication Engineering, Xi'an University of Science and Technology. His research interests include wireless communication and computer engineering.



YANG ZHOU received the B.Eng. in communication engineering from Xidian University, Xi'an, China, in 2000. Since 2000, he has been with the Ministry of Water Resources Information Center, China. His research interests include wireless communication and computer engineering.



QINGQI PEI (SM'15) received the B.Eng., M.Sc., and Ph.D. degrees in computer science and cryptography from Xidian University, in 1998, 2005, and 2008, respectively. He is currently a Professor and a member with the State Key Laboratory of Integrated Services Networks. His research interests include cognitive networks, data security, and physical layer security. He is also a Professional Member of the ACM and a Senior Member of the Chinese Institute of Electronics and the China Computer Federation.

...